Analysis of Turbulent Flow Parameters in a Motored Automotive Engine

A.E. Catania and A. Mittica
Dipartimento di Energetica - Politecnico di Torino
Turin

ABSTRACT

The turbulence quantities in the cylinder of an automotive engine with one tangential intake port were investigated, under motored conditions at 167.6 rad/s (1600 rpm), using the cycle-by-cycle nonstationary time-averaging procedure of data analysis previously developed by the authors. Correlation and spectral analysis of the engine turbulence was performed within specific time intervals during the induction and the compression strokes. Velocity data close to the cylinder wall were also analyzed in order to examine the effect of the wall on the engine turbulence in the presence of swirl.

A strong turbulence anisotropy and nonhomogeneity was observed during the induction stroke while a tendency towards isotropy and homogeneity was evident in the engine turbulence on the main part of the compression stroke.

The distributions of the micro time scale of turbulence, fluctuating about a constant value (0.2 ms) for all the measurement points, showed that the structure of the engine turbulence was virtually the same on the induction and compression strokes.

INTRODUCTION

As well known (for example [1], [2], [3], [4], [5], [6])[1], the in-cylinder turbulent flow plays a major role in reciprocating engine combustion and consequently in the engine performance and exhaust emissions. In particular, it directly influences the fuel-air mixing, the engine convective heat losses and the flame propagation process. Some experimental results on the turbulent combustion of a gaseous homogeneous mixture inside a closed vessel ([7]) indicate that the burning zone thickness and the burning velocity increase almost linearly with an increase of turbulence intensity, depending on the equivalence ratio.

Although several studies of turbulence quantities in motored engines and, more recently, in firing engines have been reported (for example [8], [9], [10], [11], [12], [13], [14], [15]), the definition of in-cylinder turbulence properties still needs further attention because of unsteadiness and cyclic fluctuation of the "mean" flow, while still more experimental data on engine turbulence is required to better understand its structure, the exact nature of its role and its correlation to the engine geometric features. An improved understanding of engine turbulence is also important for the numerical modeling of combustion processes.

The main objective of this study was to analyze the turbulence quantities in an automotive engine using the cycle-by-cycle nonstationary time-averaging procedure previously developed by the authors ([16]). The procedure allows to extract mean velocity and turbulence from the same data without including in the turbulence intensity either the cyclic fluctuation or the time varying component of the mean flow. It differs from other cycle-by-cycle data reduction methods ([8], [17], [18]), as specified in [16]. The proposed method is straightforward and of general application, including, as particular cases, the pure ensemble-averaging procedure and the conventional time-averaging data reduction method ordinarily used for the analysis of steady state turbulent flows. It can be applied to HWA[2] as well as to LDA[3] measurements if a data rate high enough to give a virtually continuous trace in every cycle is provided. The method was shown to be suitable for correlation and spectral analysis of engine turbulence, giving consistent and physically reasonable results when compared with a pure ensemble-averaging reduction of the same data ([19], [20]). In fact the turbulent fluctuation about the mean velocity according to the proposed definition can be treated as a stationary random function for specific time intervals within the engine cycle.

The analysis of HWA data acquired throughout the induction and the compression strokes along a radial direction in the cylinder of the engine was performed under motored conditions at 167.6 rad/s (1600 rpm). An induction system configuration with one tangential duct was considered. Measurements at locations very close to the cylinder wall were also performed in order to investigate the effect of the wall on turbulence in the swirling flow during the compression stroke.

Ensemble-averaged turbulence quantities were obtained from the cycle-by-cycle time-averaged values as parameters characterizing the internal gas-dynamics of the engine.

TURBULENT FLOW PARAMETER DEFINITION

The instantaneous velocity is split into a mean part and a turbulent fluctuation about this, so that, with reference to the

[1] Numbers in square brackets designate references.

[2] Hot Wire Anemometer

[3] Laser Doppler Anemometer

engine cycle i:

$$U_i(t) = \tilde{U}_i(t) + u_i(t) \tag{1}$$

where $\tilde{U}_i(t)$ is the mean velocity at time t (corresponding to the crankangle θ) and $u_i(t)$ is the velocity fluctuation about the mean.

The mean velocity curve for the cycle i is evaluated as follows. The average of the instantaneous velocity with respect to time is determined for specific time intervals within the engine cycle, and the average velocity values in the middle of the intervals are interpolated[4]. The resulting mean velocity curve is then adjusted so that the time-average value obtained therefrom in each interval is equal to the value previously determined from the instantaneous velocity in the same interval. Therefore, using the symbol $\langle f \rangle$ to represent the average of any variable $f(t)$ (or $f(\theta)$) in the time interval T (or in the crankangle interval Θ):

$$\langle f \rangle = \frac{1}{T}\int_0^T f(t+\tau)\,d\tau = \frac{1}{\Theta}\int_0^\Theta f(\theta+\varphi)\,d\varphi \tag{2}$$

we have[5]:

$$\langle U_i \rangle = \langle \tilde{U}_i \rangle \tag{3}$$

and so, from (1):

$$\langle u_i \rangle = 0 \tag{4}$$

that is the time-average of the turbulent velocity fluctuation is zero in the interval T, as it should be in agreement with the conventional definition of turbulence for a steady flow. The average turbulence intensity in T is then given by:

$$\langle u_i' \rangle = \sqrt{\langle (U_i - \tilde{U}_i)^2 \rangle} \tag{5}$$

The ensemble-averaged mean velocity $\langle U \rangle$ in the interval T is defined, for an ensemble of N records (or cycles), as:

$$\langle U \rangle = \frac{1}{N}\sum_{i=1}^{N} \langle U_i \rangle \tag{6}$$

and so the ensemble-averaged turbulence intensity in T is given by:

$$\langle u' \rangle = \sqrt{\frac{1}{N}\sum_{i=1}^{N} \langle (U_i - \tilde{U}_i)^2 \rangle} \tag{7}$$

An evaluation of the cyclic fluctuations in the mean motion can be obtained from the root-mean-square (RMS) fluctuation of the in-cycle mean velocity about the ensemble-averaged mean velocity, that is (with reference to the time-averaged values in T):

$$\langle U_{RMS} \rangle = \sqrt{\frac{1}{N}\sum_{i=1}^{N} (\langle U_i \rangle - \langle U \rangle)^2} \tag{8}$$[6]

[4] A cubic-spline was used for the interpolation, however a linear interpolation could be used as well, without any significant difference.

[5] $U_i(t)$ is considered to be a continuous function of time.

[6] A similar expression, in which U_i is replaced by u_i' and U by u', can be used for the *RMS* fluctuation of the turbulence intensity $\langle u'_{RMS} \rangle$ in the interval T.

The Eulerian time autocorrelation coefficient in the period T, starting at time t_0 (corresponding to the crankangle θ_0), is defined, in its ensemble-average form, as:

$$R(\tau) = \frac{1}{\langle u' \rangle^2}\frac{1}{N}\sum_{i=1}^{N}\left[\frac{1}{T-\tau}\int_0^{T-\tau} u_i(t)\,u_i(t+\tau)\,dt\right] \tag{9}$$[7]

where $\langle u' \rangle$ is the ensemble-averaged turbulence intensity in T; the time t is intended as relative to t_0 and the time variable τ in T ranges from 0 to $\tau_{max} = T/2$.

The normalized energy spectral density function in T is expressed, in terms of autocorrelation coefficient, as:

$$E(f) = 4\int_0^{\tau_{max}} R(\tau)\,w(\tau)\cos(2\pi f \tau)\,d\tau \tag{10}$$

where $w(\tau)$ is a window function of rectangular or Hamming type ([21]). This expression of the energy density spectrum requires that $u_i(t)$ be a stationary random function in T, which in fact it is within an approximation adequate for the purposes of the proposed method ([19]).

The micro (or dissipative) time scale of turbulence is then given by:

$$\lambda_T = 1\Big/\sqrt{2\pi^2\int_0^{f_{max}} f^2 E(f)\,df} \tag{11}$$

where f_{max} is the maximum frequency for which $E(f)$ is still finite and significant.

Because length scales of the structures characteristic of the in-cylinder turbulent flow are also of interest, it is useful to provide at least an approximate assessment of them. As for the micro length scale of turbulence in the interval T, the best that can be done at present is to evaluate it from the expression:

$$\lambda_x = \langle U \rangle \lambda_T \tag{12}$$

What can be said in support of this expression is that it is justifiable if the well known Taylor's hypotheses are satisfied, whereas even if not, it can still be considered as a more or less rough estimate of the micro length scale of turbulence in the presence of a mean flow.

Other turbulence quantities will be considered in the presentation of the experimental results, together with some comments about their definition.

HWA MEASUREMENTS

Experimental equipment and procedure

The data was taken in the single cylinder direct-injection Diesel engine reported previously ([22]), for the induction system configuration with only one of the two tangential intake ports operating (Figs. 1 and 2). Velocity measurements were performed (with a minimum modification of the engine design to introduce the probe) at five different sensor locations along a radial direction, 6 mm, 18 mm, 28 mm, 33 mm, 37 mm from the cylinder axis respectively, the latter being very close to the

[7] The expression of the autocorrelation coefficient $R_i(\tau)$ for the cycle i is simply derived from (9) by omitting the ensemble-averaging summation and substituting $\langle u' \rangle^2$ with $\langle u_i' \rangle^2$.

cylinder wall since the bore radius was 37.75 mm. The probe axis (Fig. 2a) was at a level of ≈ 3.5 mm underneath the cylinder head. Measurements at different levels were not performed due to the geometrical constraints which would have required flow disrupting modifications in the engine design to accomodate the probe. Nevertheless the probe was roughly in the middle of the relatively wide and flat combustion bowl at TDC[8], so that it was reached by the whole cylinder charge at TDC of compression. Therefore the velocity measured in the combustion bowl at the end of the compression stroke could be considered as representative of the flow of the whole charge at that stage.

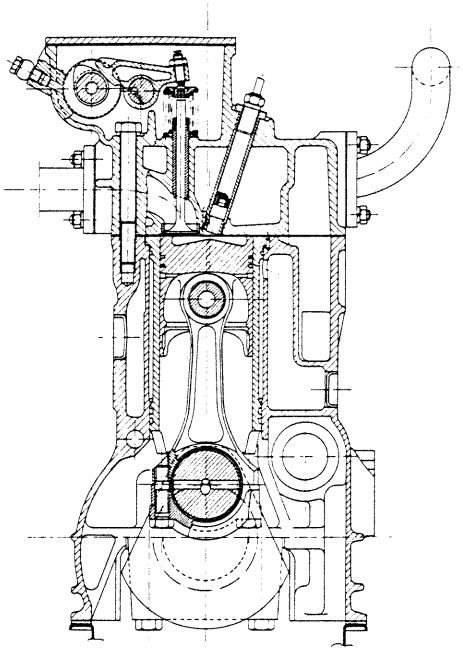

Fig. 1 – Test engine.

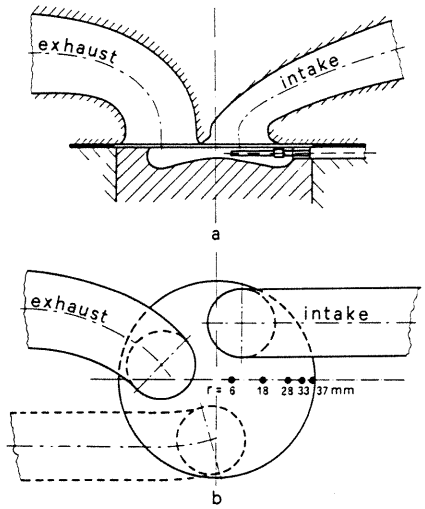

Fig. 2 – Schematic of the engine with probe setup and measurement locations.

The measuring technique and the method used for computing gas velocity from the instantaneous anemometer output voltage are those reported in [23].

A number of from thirty to fifty cycles of data[9] was recorded on analog tape for each measurement set (i.e. for each sensing wire orientation, as will be specified). A 50 kHz low-pass filter was used in recording the analog data. The analog records of pressure and temperature data were also taken, in addition to the analog records of velocity. The data was then digitized and stored in a computer file. The computation of gas velocity at each digitized point and also the analysis of the computed velocities (so as to obtain the cycle-resolved and the ensemble-averaged turbulent flow parameters) were then performed by means of an interactive computer code developed for an HP-1000, RTF-VI unit. A modified version of the algorithm developed in [24] and [25] was used for the spectrum function estimation.

At each sensor location three data sets were taken for the three different orientations of the sensing wire corresponding to the following values of the angle α between the wire axis and the cylinder axis: $\alpha = 0$, $\alpha = \pi/4$, $\alpha = \pi/2$. The squared turbulence intensity values determined for each measurement set were correlated to the squared values of the turbulence intensity components along the tangential (s), radial (r) and axial (z) directions, by means of the correlations deduced in [16][10], so as to obtain information about the directional dependence of turbulence.

Experimental uncertainties

As stated in previous papers (for example [16] and [22]) the method used for computing gas velocity from the experimental data was calibrated and tested in nonstationary as well as stationary conditions, at different gas pressures and temperatures. The tests showed a standard deviation less than ± 5%. The main sources of uncertainties in the engine measurements have been examined in references [23] and [28]. Many of them were reduced as far as possible (for example: the fouling effect was lowered by using a new wire for each set of measurements; the geometric features of the wire and weldings at prong tips were examined under microscope, so that those probes with imperfections could be removed, etc.). Based on the previous findings and on the average deviations of repeated measurement sets, a maximum uncertainty of ± 10% could be ascribed to the computed velocities. The overall experimental uncertainty, however, does not influence in any way the implications of the results and the related conclusions.

EXPERIMENTAL RESULTS

Figure 3 reports, as examples, the instantaneous velocity U_i and the corresponding mean velocity $\widetilde{U}_i$ for a typical cycle, together with the ensemble-averaged mean velocity U (as obtained within the proposed method)[11] during the in-

[8] Top Dead Center

[9] No significant advantage in taking analog records over more than thirty cycles was found.

[10] A procedure like that applied in [26] and [27] to determine the three velocity components (along the radial, the tangential and the axial directions) from the cooling velocities $U(\alpha)$ sensed by the wire for each value of α, was extended to the turbulence intensity components in [16].

[11] By simply omitting the time-average brackets $\langle\ \rangle$ we will represent the mean velocity, or any other variable, obtained by interpolating the ensemble-averaged values (made up of in-cycle time-averaged values) in the whole crankangle interval considered.

duction and compression strokes[12]. Fig. 4 shows the velocity fluctuation u_i about the mean velocity and the turbulence

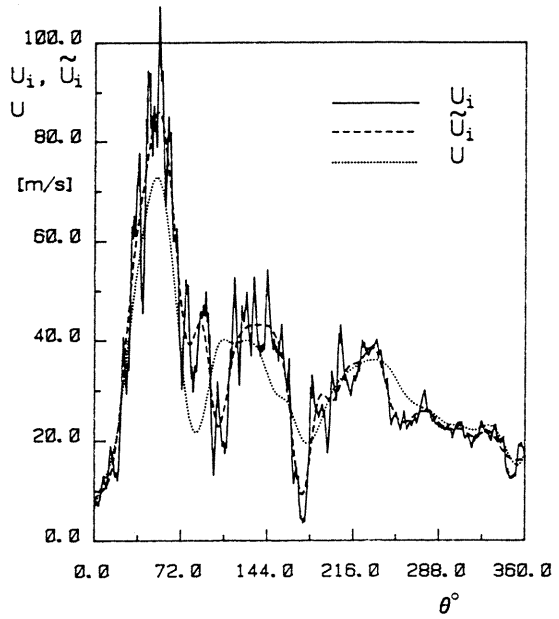

Fig. 3 – Instantaneous velocity U_i and corresponding mean velocity $\tilde{U}_i$ for a typical cycle; ensemble-averaged mean velocity U within the proposed method.

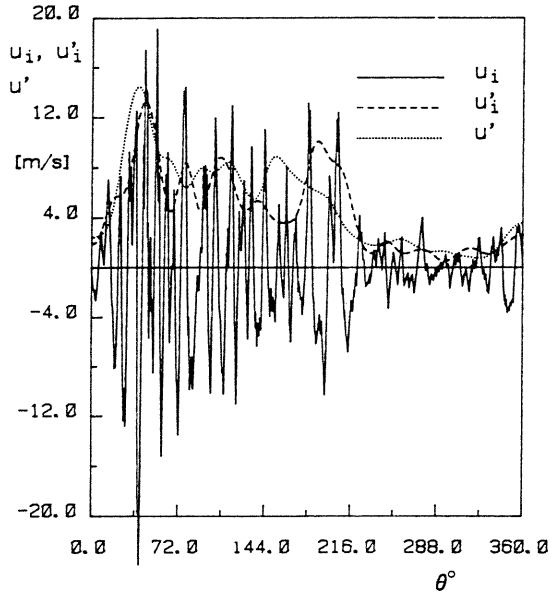

Fig. 4 – Velocity fluctuation u_i about the mean velocity and corresponding turbulence intensity u_i' for a typical cycle; ensemble-averaged turbulence intensity u' within the proposed method.

intensity u_i' for a typical cycle, together with the ensemble--averaged turbulence intensity u' (as derived from the cycle--resolved results). Both figures refer to measurements performed close to the cylinder wall ($r = 33$ mm), with the sensing wire parallel to the cylinder axis.

The period $T = 1.25$ ms (corresponding to the crankangle interval $\Theta = 12°$ at 167.6 rad/s) was used for the in-cycle time average in equation (2). This was relatively large with respect to the time scales of turbulence determined.

It is worthwhile to recall the following points emerged in [16]. The ensemble-averaged mean velocity, as well as the *RMS* fluctuation in the mean motion, did not vary significantly when the length of the averaging interval was changed, while the turbulence intensity was shown to be more sensitive to this parameter. However very short lengths yielded a rapid decrease of turbulence and increased the frequency content in the mean flow. On the other hand excessively long lengths yielded in--cycle mean velocity distributions so far from the instantaneous velocity patterns as to give rise to spurious contributions to the turbulence intensity. Therefore a range of periods was estimated, where the averaging interval could reasonably fall, as being between 0.85 and 2.0 ms.

The results on the mean flow properties within the engine considered are reported in [22] and [23], while only results on engine turbulence quantities will be presented here.

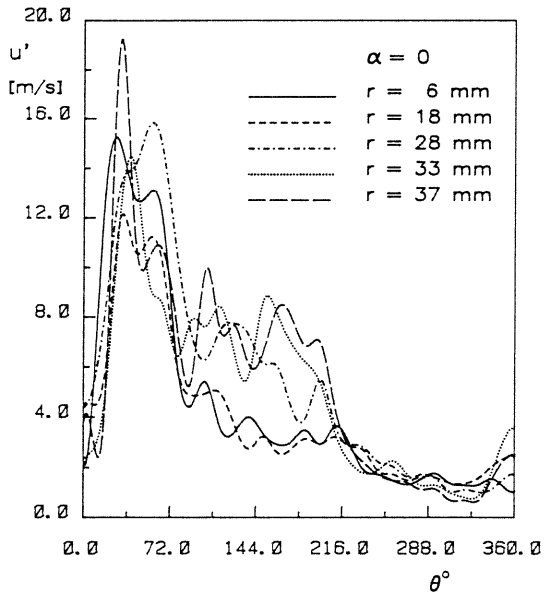

Fig. 5 – Turbulence intensity distributions.

Figures 5 and 6 show the turbulence intensity distributions vs. crankangle obtained for the wire orientations specified by the values of the angle α between the wire and cylinder axes, at the measurement points indicated by the respective values of the radius r. Considerable differences among the values of u', particularly when the wire was parallel to the cylinder axis ($\alpha = 0$), could be observed during the induction stroke, while a tendency towards homogeneity in turbulence was evident on compression. The increase in the values of u' during the last part of compression at points close to the wall ($r = 33$ mm and $r = 37$ mm) are mainly due to the fact that from $\theta = 340°$ to $\theta = 360°$ the sensing wire is accepted into a small groove machined into the piston crown to avoid interference with the probe at TDC.

The relative turbulence intensity distributions for $\alpha = 0$ (Fig. 7) showed sensible differences during the main part of the compression stroke due to the presence of swirl in the mean flow ([23]), though a small effect of turbulence nonhomogeneity could be observed at the compression end. The strong increase

[12] In this and other figures the value of the abscissa $\theta = 0°$ corresponds to the start of the induction stroke and $\theta = 360°$ corresponds to the end of the compression stroke.

of u'/U on the last part of compression at points close to the wall is due to the above mentioned groove shielding of the wire.

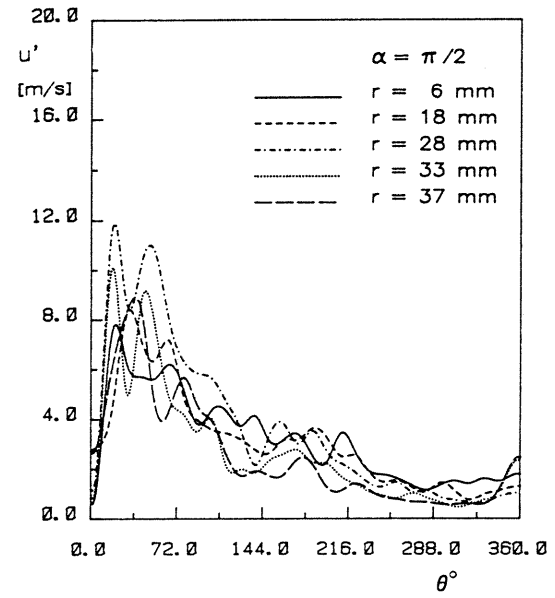

Fig. 6 – Turbulence intensity distributions.

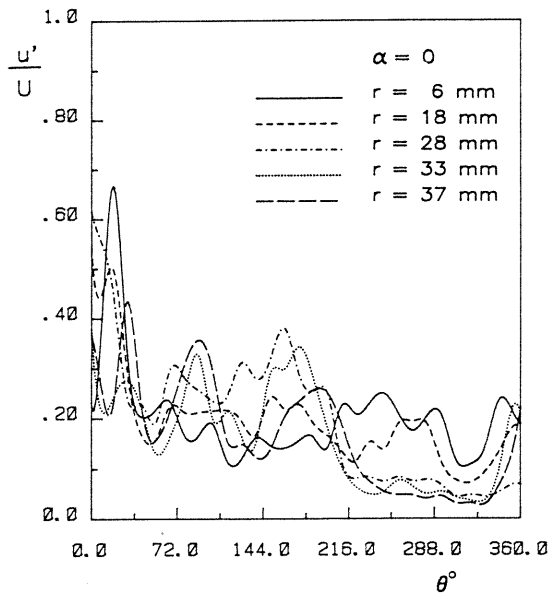

Fig. 7 – Relative turbulence intensity distributions.

Figures 8 and 9 report the cyclic fluctuation of the mean velocity and turbulence intensity respectively, the latter showing a relatively high repeatability of turbulence intensity values on compression stroke after the inlet valve closure ($\theta \approx 245°$).

Assign the simbol $u'(\alpha)$ to the turbulence intensity determined by processing the data for the wire orientation α. The values of $u'(0)$ (Fig. 5) are related to the turbulence intensity components v_s' and v_r', along the tangential and radial directions respectively, by $u'(0) \approx (v_s'^2 + v_r'^2)^{1/2}$ ([16]). The values of $u'(\frac{\pi}{2})$ (Fig. 6) can be expressed as $u'(\frac{\pi}{2}) \approx (v_r'^2 + v_z'^2)^{1/2}$, v_z' being the turbulence intensity along the axial direction. Based on these relations, a strong turbulence anisotropy during the early part of induction and a tendency towards isotropy on the main part of compression could also be deduced from

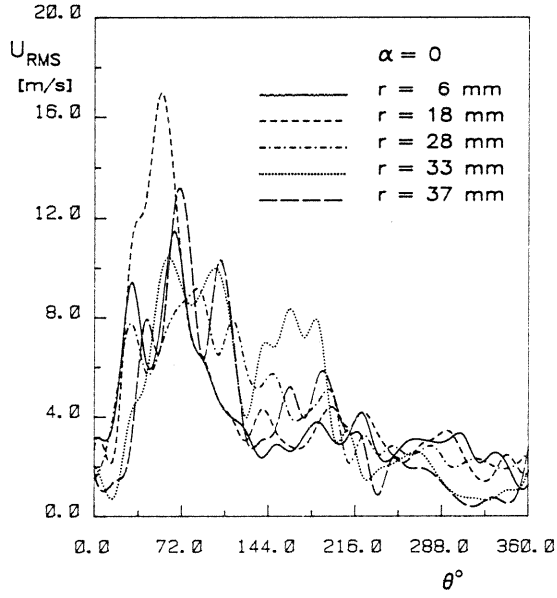

Fig. 8 – Distributions of *RMS* fluctuation of the mean velocity.

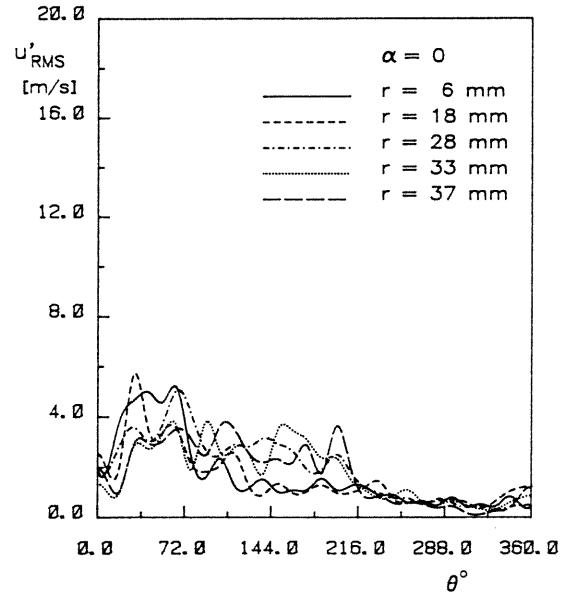

Fig. 9 – Distributions of *RMS* fluctuation of the turbulence intensity.

the results of Figs. 5 and 6, for all the measurement points considered. A considerable anisotropy was still present during the last part of induction and the early part of compression at points farther from the cylinder axis ($r \geqslant 28$ mm), where a prevailing tangential turbulence component was present. The same conclusions on the directional dependence of turbulence as derived above are confirmed by the distributions of $k_1 = v_s'^2 - v_z'^2$ given in Fig. 10, as well as by the distributions of the ensemble averaged turbulence shear stress (per unit density) $k_2 = -v_s v_z$ (Fig. 11) as obtained from the correlations reported in [16]. It shoud be pointed out that while it was possible to extract the three components of the mean velocity from

the cooling velocities obtained by processing the HWA data for the three values of α: $0, \frac{\pi}{4}$ and $\frac{\pi}{2}$ ([23]), it was not possible to separate the three components of the turbulence intensity completely, owing to the presence of the shear stress.

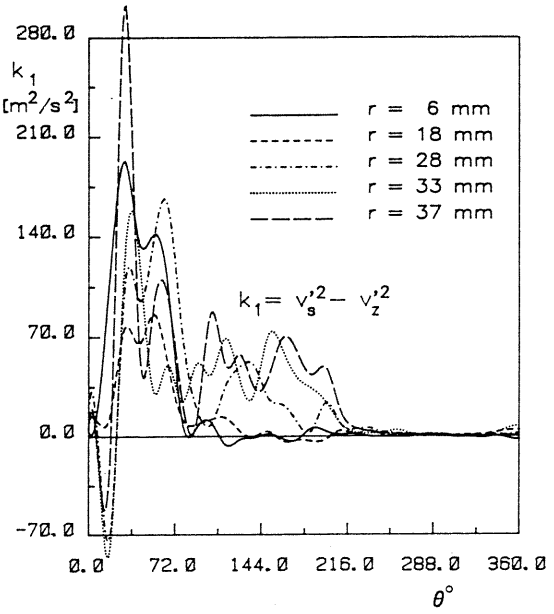

Fig. 10 – Distributions of the difference (k_1) between the squared turbulence intensity components along the tangential and the axial directions.

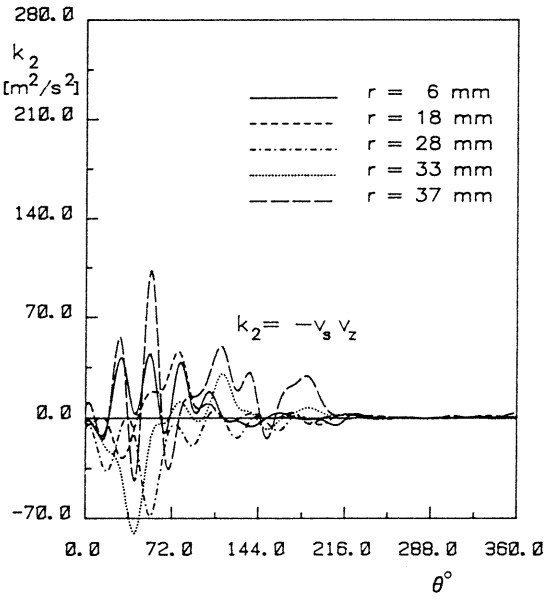

Fig. 11 – Distributions of the ensemble averaged turbulence shear stress k_2 (per unit density).

Measurements for the three values of α, but with the probe axis along the other two directions would have been required in order to evaluate separately the ensemble-averaged values of all the turbulence stresses per unit density.

Figure 12 shows the autocorrelation coefficient R, as a function of the crankangle $\theta - \theta_0$, obtained for $\theta_0 = 60°$, using the period $T = 3.125$ ms (corresponding to the crankangle $\Phi = 30°$) as the correlation interval in equation (9). The patterns of R were typical of wide band random functions ([29]). Fig. 13 reports the normalized energy spectral density functions corresponding to the correlation coefficients of Fig. 12. The highest contribution to the turbulent energy occurred at approximately the same frequency for all the measurement points (as evident in Fig. 13) and also for all the correlation intervals on the induction and compression strokes, as well as for all the wire orientations, as can be deduced from the distributions of λ_T vs. crankangle in Figs. 14 and 15. The micro time scale of turbulence, evaluated either from expression (11) or from the intersection of the abscissa axis with the osculating parabola in the vertex of the correlation curve, was nearly insensitive to the length of the correlation interval within certain limits ([19] and [20]). A crankangle interval of

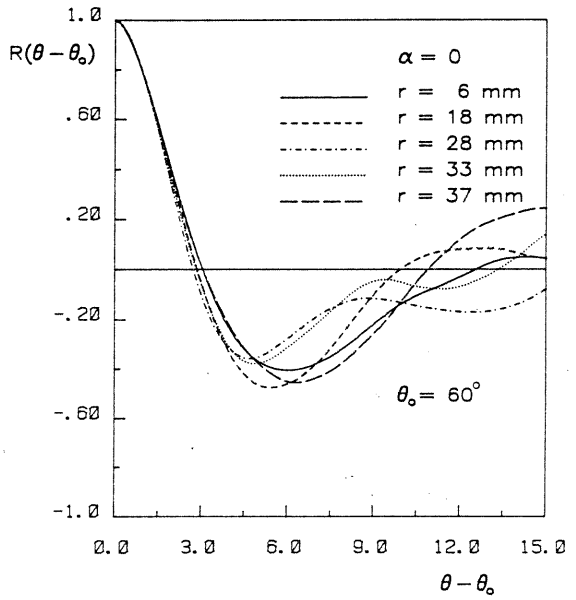

Fig. 12 – Autocorrelation coefficient.

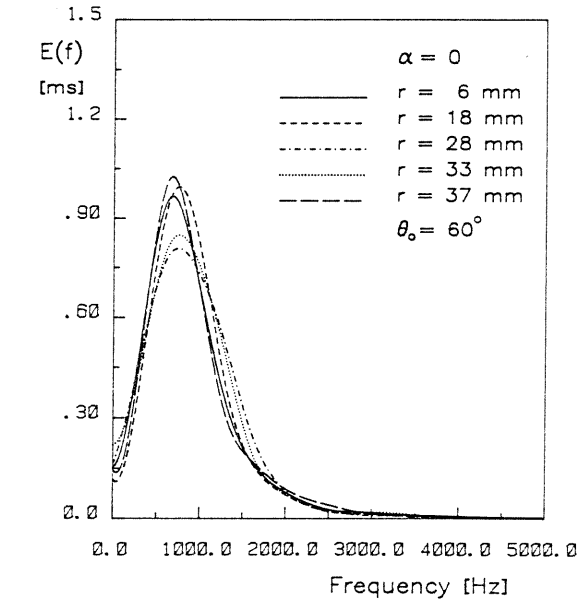

Fig. 13 – Normalized energy spectral density function.

30° was chosen for the correlation in Fig. 12 in order to give better evidence of the patterns of the autocorrelation coefficient which is in fact represented in only half of that interval.

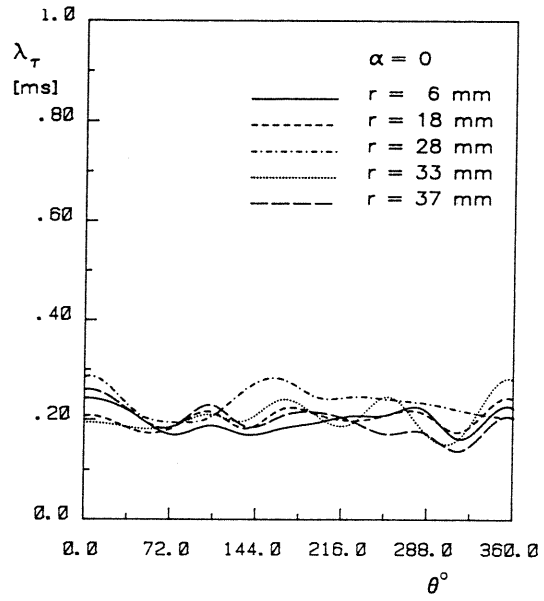

Fig. 14 — Distributions of the micro time scale of turbulence.

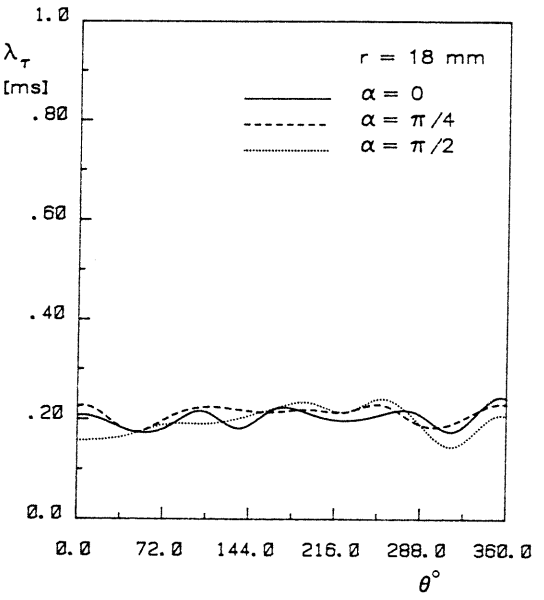

Fig. 15 — Distributions of the micro time scale of turbulence.

From the distributions of λ_T obtained it could be inferred that the structure of the engine turbulence was virtually uniform in the central core of the flow, as well as very close to the cylinder wall and furthermore was nearly the same during the induction and compression strokes. The results on the mean flow ([23]) showed the presence of a secondary jet flow in the clockwise direction (Fig. 2) at the measurement points on the induction stroke and the presence of a counterclockwise swirling flow, that is the main flow, on compression stroke. Therefore the structure of turbulence in both flows was roughly the same, the wall effect being very small.

Evaluation of the micro length scale of turbulence by means of equation (12) could be justified, as a first order approximation, at least on the part of the compression stroke after the inlet valve closure. However even then the hypothesis of uniform mean velocity in the flow field is not satisfied, owing to the presence of swirl, and also the relative turbulence intensity could not be considered as very small with respect to unity. Nevertheless, based on a mean value of the bulk flow velocity on the main part of compression ([23]) a rough estimate of the micro length scale of turbulence in the engine cylinder after the inlet valve closure could be $\lambda_x \approx 3.0\text{-}4.0$ mm.

As for the integral time scale of turbulence, the conventional definition ([30]) could not be used, owing to the pattern of the autocorrelation coefficient shown in Fig. 12, as also evident from the values of $E(0)$ in Fig. 13. Therefore the definition of the integral time scale of turbulence still needs further attention.

CONCLUDING REMARKS

The cycle-by-cycle nonstationary time-averaging procedure of data analysis previously developed by the authors was applied to the investigation of turbulence quantities in the cylinder of an automotive engine. The procedure allows extraction of the mean velocity and turbulence intensity from the same data without including in the latter either the cyclic fluctuation of the mean velocity or its time varying component.

Correlation and spectral analysis of the engine turbulence was performed within specific time intervals during the induction and compression strokes. In fact the turbulent fluctuation about the mean velocity, as defined within the proposed method, could be treated as a stationary random function in each correlation interval.

Velocity data close to the cylinder wall was also analyzed in order to examine the effect of the wall on the engine turbulence in the presence of swirl.

The following main points emerged from the analysis of HWA data, acquired throughout the induction and compression strokes along a radial direction in the cylinder of the engine motored at 167.6 rad/s, for the induction system configuration with one tangential port.

A strong turbulence anisotropy during the early part of induction and a tendency towards isotropy on the main part of compression was found for all the measurement points considered. The anisotropy observed at points close to the cylinder wall on the last part of induction and the early part of compression was due to a prevailing tangential component of turbulence intensity.

A nonhomogeneity in turbulence existed during the induction stroke while a tendency towards homogeneity was evident on the compression stroke.

The distributions of the micro time scale of turbulence, fluctuating about a constant value (0.2 ms) for all the measurement points, showed that the structure of the engine turbulence was virtually the same on both the induction and compression strokes, in the secondary jet flow, as well as in the main flow, the effect of the wall being very small.

A rough estimate of the micro length scale of turbulence in the engine cylinder on the main part of compression, could be considered as 3.0-4.0 mm, based an a mean value of the bulk flow velocity.

ACKNOWLEDGMENT

This work has been financially supported by M.P.I. (Ministero della Pubblica Istruzione) under 40% fund.

REFERENCES

1 D.R. Lancaster et al., "Effects of Turbulence on Spark-Ignition Engine Combustion", SAE paper 760160.

2 F.W. Huber, "Influence of Mixture Formation on the Efficiency of a Diesel Engine with Direct Injection", MTZ, March 1976.

3 F. Brandl et al., "Turbulent Air Flow in the Combustion Bowl of a D.I. Diesel Engine and Its Effect on Engine Performance", SAE paper 790040.

4 M.L. Monaghan, H.P. Pettifer, "Air Motion and Its Effect on Diesel Performance and Emissions", SAE paper 810255.

5 J.R. Smith, "The Influence of Turbulence on Flame Structure in an Engine", Symposium on Flows in I.C. Engine, ASME WAM 1982.

6 M. Shimoda et al., "Effect of Combustion Chamber Configuration on In-Cylinder Air Motion and Combustion Characteristics of D.I. Diesel Engine", SAE paper 850070.

7 Y. Hamamoto et al., "Effects of Turbulence on Combustion of Homogeneous Mixture of Fuel and Air in Closed Vessel", Bulletin of JSME, Vol. 27, No. 226, pp. 756-762, 1984.

8 D.R. Lancaster, "Effects of Engine Variables on Turbulence in a Spark-Ignition Engine", SAE paper 760159.

9 P.O. Witze, "Measurements of the Spatial Distribution and Engine Speed Dependence of Turbulent Air Motion in an I.C. Engine", SAE paper 770220.

10 M. Haghgooie et al., "Turbulent Time-Scale Measurements in a Spark-Ignition Engine Using Hot Wire Anemometry and Fast Response Ion Probes", Symposium on Flows in I.C. Engines, ASME WAM 1982.

11 T. Wakisaka et al., "Turbulence Structure of Air Swirl in Reciprocating Engine Cylinders", Symposium on Flows in I.C. Engines, ASME WAM 1982.

12 M.J. Tindal et al., "The Effect of Inlet Port Design on Cylinder Gas Motion in Direct Injection Diesel Engines", Symposium on Flows in I.C. Engines, ASME WAM 1982.

13 J.C. Dent and N.S. Salama, "The Measurement of the Turbulence Characteristics in an Internal Combustion Engine Cylinder", SAE paper 750886.

14 C. Arcoumanis et al., "Squish and Swirl-Squish Interaction in Motored Model Engines", JFE, Vol. 105, pp. 105--112, 1983.

15 J.K. Martin et al., "Combustion Effects on the Preflame Flow Field in a Research Engine", SAE paper 850122.

16 A.E. Catania, A. Mittica, "A Contribution to the Definition and Measurement of Turbulence in a Reciprocating I.C. Engine", ASME Diesel & Gas Engines Symposium, ETCE, 1985.

17 R.B. Rask, "Comparison of Window, Smoothed-Ensemble, and Cycle-by-Cycle Data Reduction Techniques for Laser Doppler Anemometer Measurements of In-Cylinder Velocity", Symposium on Fluid Mechanics of Combustion Systems, ASME FED Spring Meeting 1981.

18 T.M. Liou and D.A. Santavicca, "Cycle Resolved LDV Measurements in a Motored I.C. Engine", Symposium on Engineering Applications of Laser Velocimetry, ASME WAM 1982.

19 A.E. Catania, A. Mittica, "Problems of Turbulent Flow Parameter Definition and Measurement in a Reciprocating I.C. Engine", IEA VI Task Leaders Conference, Asilomar, 1984.

20 A.E. Catania, A. Mittica, "Cycle-by-Cycle, Correlation and Spectral Analysis of I.C. Engine Turbulence", Pubbl. N. DE 057/MA, 1985.

21 A. Papoulis, "Signal Analysis", McGraw-Hill, 1984.

22 A.E. Catania, "Induction System Effects on the Fluid--Dynamics of a D.I. Automotive Diesel Engine", ASME Diesel & Gas Engines Symposium, ETCE, 1985.

23 A.E. Catania, "3-D Swirling Flows in an Open-Chamber Automotive Diesel Engine with Different Induction Systems", Symposium on Flows in I.C. Engines, ASME WAM 1982.

24 C.M. Rader, "An Improved Algorithm for High Speed Autocorrelation with Applications to Spectral Estimation", IEEE Trans. Audio Electroacoustics, Vol. AU-18, No. 4, 1970.

25 L.R. Rabiner et al., "Correlation Method for Power Spectrum Estimation", IEEE Programs for Digital Signal Processing, 1979.

26 K.H. Huebner and A.T. McDonald, "A Dynamic Model and Measurement Technique for Studying Induction Air Swirl in an Engine Cylinder", Journal of Engineering for Power, April 1970.

27 A.E. Catania, "Air Flow Investigation in the Open Combustion Chamber of a High-Speed, Four-Stroke Diesel Engine", ASME paper 80-FE-5.

28 A.E. Catania, "Repeatability and Uncertainty Analysis of Hot-Wire Measurements in a High Compression-Ratio, High Speed Motored Engine", Pubbl. N. 219 IMPT 1979 (in Italian).

29 J.S. Bendat, A.G. Piersol, "Engineering Applications of Correlation and Spectral Analysis", John Wiley & Sons, 1980.

30 J.O. Hinze, "Turbulence", McGraw-Hill, 1975.